



A comparative study of nano magnesium oxide versus platelets rich fibrin to repair the induced radial fracture in dogs

Y.F. Abdulmawjood and M.G. Thanoon 

Department of Surgery and Theriogenology, College of Veterinary Medicine, University of Mosul, Mosul, Iraq

Article information

Article history:

Received June 12, 2021
Accepted October 15, 2021
Available online February 24, 2022

Keywords:

Dog
Fracture
Radial bone
PRF
NMO

Correspondence:

M.G. Thanoon
moyaserthanoon@uomosul.edu.iq

Abstract

This project evaluated the effects of nano magnesium oxide versus platelets rich fibrin on induced radial fracture bone healing. Eighteen males and non-pregnant females of adult local stray dogs, weighing 17.6 ± 0.8 kg and aged 2.0 ± 0.1 years, were used. These trials animals were randomly divided into three groups of equal numbers. In the first group, control group (C), a transverse radial fracture was induced then immobilized by external fixation as gypsum. In this group, the fracture line was not treated with any bioactive material. In the second group, platelets rich fibrin group (PRF), the fracture line was treated by adding platelets rich fibrin. In the third group, nano magnesium oxide (NMO), the fracture line was treated by adding a suspension of nano magnesium oxide. The radiographic results showed that the fractured bone healing was faster in the second group than in the first and third groups, while the third group was better than the first group. The concentration rates of serum calcium and alkaline phosphatase were increased in the weeks followed the surgical operation. Depending on the radiographic pictures and serial rates of alkaline phosphatase, the second PRF and the third NMO groups were the better-fractured bone healing than the first one. In conclusion, this study revealed that using each platelets rich fibrin and nano magnesium oxide enhanced and improved the healing of the induced radial fracture.

DOI: [10.33899/ijvs.2021.130500.1836](https://doi.org/10.33899/ijvs.2021.130500.1836), ©Authors, 2022, College of Veterinary Medicine, University of Mosul.
This is an open access article under the CC BY 4.0 license (<http://creativecommons.org/licenses/by/4.0/>).

Introduction

Claudication in dogs is a widespread injury, and it can be defined as abnormal posture or walking resulting from a defect or disorder in the formation of the skeleton or impairment of the locomotor system. Among the leading causes of lameness in animals, especially dogs are congenital anomalies, accidental traffic or falls from high places, and fighting with other animals or gunshots and explosions. Locomotor disorders are considered among the most common causes leading to lameness in dogs (1). Antebrachium fractures, including the radius and ulna bones, are the third most public fracture in dogs, accounting for approximately 17% of all fractures afflict, and the Pomeranian dogs are more likely to suffer forearm fractures (2). This relatively high rate of fracture occurrence, especially for radius, is because it represents the most

significant part of the forearm area, where the heaviest weight falls on it. Therefore, it is the bone most susceptible to fractures than the rest of the forelimb bones (3). Another fact about the radius fracture is that it represents long bones fractures that often take a long time to heal compared to the rest of body bones due to the lack of good blood supply and the shortage of dense connective tissue. Therefore, the delay in healing or failure is the common and most expected result (4). Fracture bone healing is a rare regenerative process that leads to the complete restoration of the fractured bone to its normal shape and function. The healing of the fractured bone is a complex process consisting of multiple and sequential stages and requires a coordinated interaction between the different cells, growth factors, and cytokines with the availability and appropriate mechanical conditions surrounding the fracture (5). The term nanomaterial technology was first used in the middle of the last century in

1959. Nanomaterial technology has become one of the most prominent techniques used in various engineering and life disciplines. Nanotechnology is the technology that deals with materials at the level of atoms and molecules within the range of the nanometer scale. Nanomaterials have many unique properties compared to conventional materials, including their possession of a much larger surface area than their size (6,7). Nanomaterials have been applied and introduced in many research disciplines, including biomedical sciences, where the nanomaterials simulated natural tissues by providing the appropriate extracellular environment for cells to survive and grow within the material. There was a great need to use nanomaterials suitable for repairing major defects in fractured bones (8). For many years, Magnesium oxide (MgO) of different weight fractions has been broadly used as a bioactive material for orthopedic implantation due to its excellent biocompatibility, superior mechanical strength, and ability to improve bone density (9). Besides, fracture toughness improves up to 50% with using of nano MgO particles (10,11). Other researchers found that using MgO will hasten bone formation by stimulating more active osteogenesis in vivo osteocalcin and type I collagen synthesis (12). Magnesium is considered a biocompatible, low-cost mineral and is naturally present in the body tissue, approximately 1% of the bone mass. In the field of orthopedics, magnesium alloys have been extensively studied. It has been proven that magnesium promotes and accelerates bone growth as it enhances and accelerates the effectiveness of osteoblasts and its indirect effect on mineral metabolism by activating alkaline phosphatase. It also shows a substantial role in modulating the functions of cells by making them tend to adhesion, proliferation, and migration. The magnesium is biodegradable quickly in the body and releases hydrogen gas, which will change the microenvironment in body fluids to either acidic or alkaline. With regard to nano-MgO, which is dispersed in a polymer, can release magnesium ions slowly to promote the formation of bone tissue and avoid the adverse reaction that harms the body's cells (13). The beneficial influence of MgO could also help prevent orthopedic and dental infections due to its antimicrobial (14). Platelet-rich fibrin (PRF) is the second generation of concentrated platelets because the first generation is platelet-rich plasma. The concentrated platelets of platelet-rich fibrin are founded in the complex fibrin matrix (15). Platelet-rich fibrin has many biological benefits, as it is used to enhance the healing process of soft and hard tissues and a scaffold to bridge cavities and defects of soft and hard tissues, such as accelerate the fractured bone healing (16). The beneficial influences of platelet-rich fibrin RPF for osseous regeneration, especially the early beginning of trabecular bone formation, and the elevation in bone mineral density and volume make it considered a new novel tool (17). The therapeutic properties of this relatively recent biotechnology have been used extensively to hasten soft tissue and bone healing for many different fields, especially sport medicine

and orthopedics. The secret behind its importance is because of its ability to ongoing locally and regularly providing of a wide range of growth factors, cytokines, and proteins that mimic reparative tissue process (18), that when used for the treatment of bone defects, improves bone mineral density, bone formation and even bone volume (19).

Materials and methods

This study used 18 animals weighing 17.6 ± 0.8 kg and aged 2.08 ± 0.13 years of both male and nonpregnant female stray dogs, which were healthy. These animals were kept in the animals' husbandry belongs to Veterinary Medicine College, University of Mosul, under the same feeding and management conditions. All dogs were treated against internal and external parasites using Ivermectin 1% at a dose of 0.2-0.4 mg/kg BW subcutaneously and repeated after 14 days before surgical intervention. The trial animals were randomly distributed into three groups of equal numbers. The first one is the control group (C), while the second is platelets rich fibrin group (PRF), and the third is the nano magnesium oxide group (NMO). Before the surgery, the experimental animal starved for 24 hours, and the water was free access.

The surgical operations were performed under general anesthesia, by intramuscular injection of Ketamine hydrochloride 10% at a dose 15 mg/kg BW mixed with Xylazine hydrochloride 2% at a dose 5 mg/kg BW preceded about 10 minutes by intramuscular injection of Atropine sulfate 1% at a dose 0.04 mg/kg BW. Under the aseptic surgical technique, all trial animals underwent transverse radial fracture using a wire saw, then immobilized this fractured bone by external fixation using Plaster of Paris. In the first group (C), no adding any substance to the fracture line, while in the second group (PRF) adding the platelet-rich fibrin which was prepared previously from the same animal, finally the third group (NMO), the fracture line was treated with 20 μ g suspension of nano magnesium oxide. The platelet-rich fibrin was prepared immediately before the surgical operation by drawing 10 ml of whole blood from the cephalic vein of the same surgical operated animal, then centrifugation of this fresh blood without anticoagulants at 3000 rpm for 10 minutes. After centrifugation, we got a tube of three distinct layers. The top layer was the poor platelets plasma, while the middle one was the platelets rich in fibrin separated by surgical scissors from the bottom layer of red blood cells (Figure 1) (20). This study used magnesium oxide nanopowder 99% of average particle size (APS) 20nm with specific surface area (SSA) 60 m²/g from US research nanomaterials, Inc. The radial fracture line of the third group (NMO) was treated with 20 μ g of nano magnesium oxide suspension, which was prepared by weighing 100 μ g of magnesium oxide nanopowder then dissolved in 10 ml of distilled water after that taken 2 ml of this suspension to add on the fracture line.

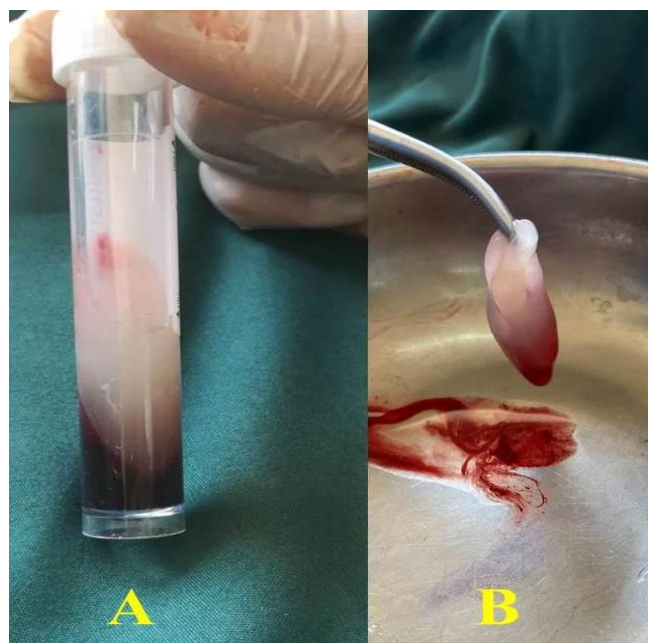


Figure 1: Shows platelets rich fibrin preparation. A: The completed centrifuged test tube showing its three distinct layers, the uppermost layer is poor platelets plasma, the medium layer is the PRF, while the lowermost one is the red blood cells. B: Extraction of PRF from the centrifuged test tube by surgical forceps following detaching PRF layer from bottom RBC layer by surgical scissors.

Post-operative care; for five successive days, intramuscular administration of penicillin-streptomycin at a dose of 10000 IU, 20 mg/kg BW, was applied respectively and a daily wound dressing. The thread stitches were removed at 10-12 days following the operation. Daily physical examination of all experimental animals for two weeks, then weekly till the end of experimental study (follow up ten weeks). The radiological investigation of fractured bone immediately started by taking a plain radiographic image following surgery to ensure both fractured ends were aligned. A follow-up x-ray examination was performed every two weeks until the end of the study.

The whole calcium and alkaline phosphatase enzyme levels were measured by the colorimetric method by using a Calcium 3L79 kit from Abbott GmbH & Co. KG for calcium and a (Cobas®) kit from Roche Company for alkaline phosphatase enzyme. Blood samples were collected at zero earlier to surgery, then at 2, 4, 6, 8 weeks following operation from all experimental animals. Sigma Stat (Jandel scientific software V3.1), at a level of probability less than 0.05 ($P < 0.05$), was used for statistical analysis of our results data.

Results

All experimental animals showed partial loss of appetite post-operatively, then the normal appetite for food had

returned after 3-4 days of surgery. The external wound of the fractured limb was healed in 8-10 days after the operation, without any serious complications, just slight redness and swelling, which retarded after 3-4 days. All trial animals looked like a limp after surgical operation by lifting the fractured limb from the second day till the first week post-surgical operation. The claudication was evident in animals of the first group until the third week post-operation, but the lameness in the third group was less apparent at the end of week two after the operation. In contrast, the animals of the PRF group exhibited an ability to bear their body weight on the fractured extremity at the end of week three following the operation.

The biochemical markers outcomes indicated an elevation in total serum calcium and alkaline phosphatase concentration levels at the weeks following surgery. These outcomes with their statistical analysis are summarized in table 1 for calcium rates and table 2 for alkaline phosphatase. The radiographical pictures that showed and confirmed the fracture healing process was faster and much better in the second group incomparable comparison to the first and third groups. The findings of radiographical data for the three groups are displayed in table 3.

Table 1: Mean of calcium concentration levels (mg/dL) with its statistical analysis in the three experimental main groups

Time	C group	PRF group	NMO group
0W	10.6±0.2 ^a	10.8±0.1 ^a	10.7±0.2 ^a
2W	11.2±0.3 ^a	12.5±0.3 ^b	11.8±0.3 ^b
4W	11.7±0.2 ^a	12.7±0.2 ^b	12.6±0.2 ^c
6W	11.4±0.2 ^a	12.0±0.2 ^a	11.9±0.2 ^a
8W	11.5±0.2 ^a	11.6±0.1 ^a	11.1±0.1 ^a

The symbol 0W represents the time before the surgical operation, and the symbols 2W, 4W, 6W, and 8W represent the weeks following surgery. The different small letters (a-c) show the significant difference between the three experimental groups ($P < 0.05$).

Table 2: Mean of alkaline phosphatase concentration (U/dL) with its statistical analysis at the three main experimental groups

Time	C group	PRF group	NMO group
0W	19.3±0.5 ^a	18.6±0.6 ^a	20.1±0.6 ^a
2W	19.3±0.3 ^a	23.1±1.1 ^b	20.6±0.8 ^a
4W	20.4±0.5 ^a	26.5±0.6 ^b	21.9±1.0 ^c
6W	23.8±0.6 ^a	30.5±0.9 ^b	27.7±0.9 ^c
8W	21.9±0.9 ^a	28.4±0.9 ^b	24.4±1.5 ^b

The symbol 0W represents the time before the surgical operation, and the symbol 2W, 4W, 6W, and 8W represents the time in weeks following the surgical operation. The different small letters (a-c) indicate the significant difference between the three groups ($P < 0.05$).

Table 3: Shows x-ray finding of first group C, second group PRF, and third group NMO

Week	C group	PRF group	NMO group
2	There is no evidence of periosteal reaction-clear fracture line (Figure 2-C)	There is some periosteum reaction-clear fracture line (Figure 2-PRF)	There is a slight periosteum reaction-a clear fracture line (Figure 2-NMO)
4	There is some periosteum reaction with little callus formation-clear fracture Line (Figure 3-C)	An increase in callus mass formation and a partially crossed fracture line. The fracture line is less pronounced (Figure 3-PRF)	There is evidence of callus formation with started to bridge fracture line. The fracture line is semi-clear (Figure 3-NMO)
6	An elevation in callus size formation with partial bridged the fracture line. The fracture line is semi-clear (Figure 4-C)	The callus formation increased in size and bridged more than half of the fracture line. The fracture line partially disappeared (Figure 4-PRF)	The callus formation increased in size and partially bridged the fracture line. The fracture line is less noticeable (Figure 4-NMO)
8	A growing callus formation around the fracture site with a bridged fracture line. The fracture line partially disappeared (Figure 5-C)	The fractured bone has become nearly normal shape, with a drop-in callus mass around the fracture site (Figure 5-PRF)	The shape of the fractured bone became semi-normal, with a small callus around the fracture site (Figure 5-NMO)
10	The fractured bone looked like a standard shape. The fracture line disappeared with little callus around the fracture site (Figure 6-C)	The fractured bone seems normal in shape (Figure 6-PRF)	The fractured bone is nearly normal shaped with very little callus at the fracture site (Figure 6-NMO)



Figure 2: Radiographic picture of dog fractured radius bone at the second week after the operation. There is no evidence of periosteal reaction (arrow) in the first group (C), while there is some periosteum reaction (arrows) in the second group (PRF) and less than it in the third group (NMO). The fracture line is evident in all experimental groups.



Figure 3: Radiographic picture of dog fractured radius bone at the fourth week following surgery. The periosteum in the second group (PRF) started to bridge fracture line (arrow), there is evidence of periosteal reaction (arrow) in the third group (NMO), while in the first group (C), there is some periosteum reaction (arrow). The fracture line is semi-clear in all experimental groups.



Figure 4: Radiographic picture of dog fractured radius bone at the sixth week following surgery. In the first group (C), the callus formation started to bridge the fracture line (arrow), with a semi-clear fracture line; but the callus formation partially bridged the fracture line (arrow) in the third group (NMO), the fracture line is less pronounced; while in the second group (PRF) the callus formation crossed more than half of the fracture line (arrow), the fracture line partially disappeared.

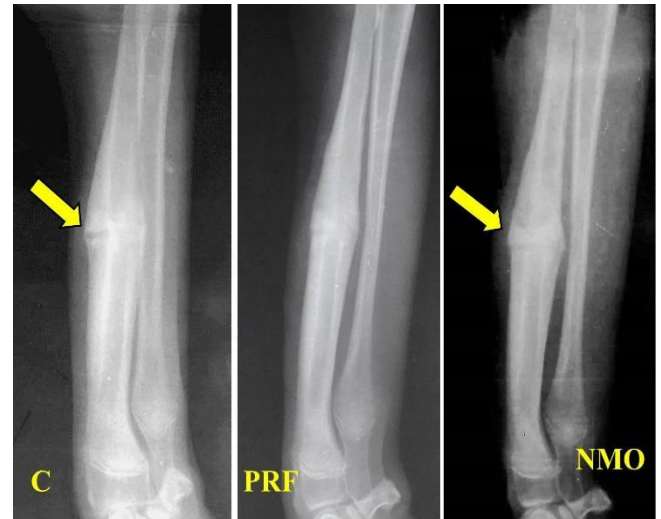


Figure 6: Radiographic picture of dog fractured radius bone at the tenth week following surgery. In the first group (C), the fractured bone looked almost normal in shape. The fracture line disappeared with little callus around the fracture site (arrow); in the second group (PRF), the fractured bone appears normal in shape; while in the third group (NMO), the fractured bone nearly has a typical shape with very little callus at the fracture site (arrow).

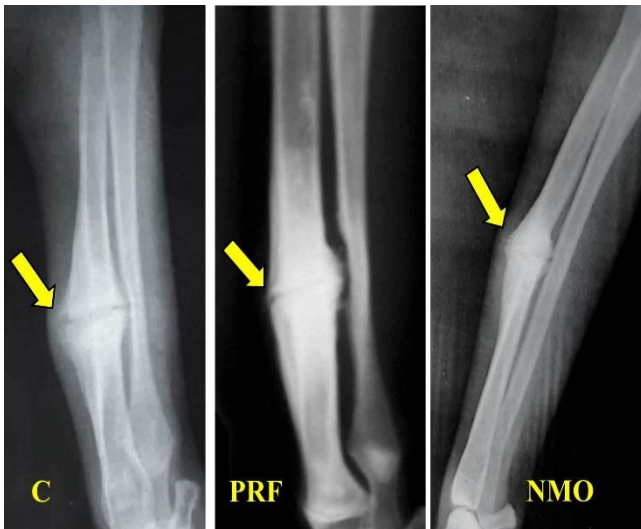


Figure 5: Radiographic picture of dog fractured radius bone at the eighth week after the operation. In the first group (C), a rise in callus formation around the fracture site with a bridged fracture line (arrow) appeared. The fracture line partially disappeared; and in the second group (PRF), the fractured bone has become nearly normal in shape, with drop-in callus size around the fracture site (arrow); while in the third group (NMO), the shape of fractured bone became semi-normal, with having a nominal size of callus around the fracture site.

Discussion

All trial dogs showed signs of partial loss of appetite with redness and mild swelling at the operation site for 3-5 days following the operation. These clinical signs were subsided within 5-7 days after the operation. These results coincide with Tomlin *et al.* (21), who said that the most frequent clinical sign of radio-carpal bone fracture is soft-tissue swelling. All experimental animals experienced lameness after surgical operation. The claudication was evident at weeks 1 and 2 after the operation, then little pronounced at weeks 3 and 4. The lameness was disappearing at the fifth and sixth weeks after the operation, and these signs of lameness agree with Gwyneth and Noel (2), who said that the external coaptation was responsible for minor complications of intermittent lameness.

The radiographic results of the second week after operation; showed that the fracture line was noticeable in all experimental animals. Despite that, the second group (PRF) showed some periosteum reaction more than the third group (NMO), while the less periosteum reaction was in the first group. The periosteum reaction was more evident in the second group (PRF) than in the third group (NMO). This may be due to platelets rich fibrin, which added to the fracture line in the second group. This coincides with Bai *et al.* (22); and Dohan *et al.* (23), who said that the fibrin matrix, unlike other concentrated platelets, would be able to progressively release cytokines and chemokines, which have an essential function in the stimulation, migration, and

proliferation of cells at the first hours of adding it to the affected inflammatory part of the body.

On the other hand, the third group showed better periosteum reaction than the first group. This may be due to the fracture line in the third group was treated by adding nano-magnesium oxide. In contrast, the fracture line in the first group was not treated with any bioactive materials, which agrees with Griffin *et al.* (24). They said that the nanomaterials, with features on the Nanoscale, can provide the appropriate matrix environment to guide cell adhesion, migration, and differentiation, which is why the first group suffers from the less periosteum reaction.

In the fourth week following the operation, the second group showed growth in callus size construction with partially bridged the fracture line, whereas a bit of callus formation with a clear fracture line in the first group. This difference between the second and the first group, in addition to apparent progression in the size of the callus formation in the second group, may be attributed to the role of platelet-rich fibrin, which was added to the fracture line in the second group, while the fracture line in the first group was not treated with any bioactive substance. This agreement with Khiste and Naik Tari (25), who said that the presence of fibrin in the platelets rich fibrin, which is considered the activated form of fibrinogen, plays essential roles in platelet aggregation and achieving hemostasis also act as a scaffold to fill gaps in the soft and hard tissues. Also, the fibrin matrix can consistently release angiogenic, hemostatic, and osteoconductive properties. Also, there is no significant difference between the second and third groups in the size of callus formation, while there is a statistically significant difference between the third and first groups because the callus formation was more significant in the third group than that formed in the first. This coincides with Wang (26), who said that the nanomaterial encourages vascularization and new bone formation and allows early cellular infiltration and later integration with native tissue by mimicking nanoscale features of bones offering exceptional features.

The radiographic pictures of the sixth-week post-surgery; revealed an advancement of the second group over the first group; that represented by an increase in the size of callus mass presence, which crossed the fracture line in the second group, while in group no.1 there was increasing in the callus mass but with partially bridged the fracture line, therefore the fracture line was semi-clear. These differences in both groups may be due to the treatment of fracture line in the second group by platelet-rich fibrin. The platelet-rich fibrin is considered a rich supply of autologous cytokines and growth factors. This agrees with Serafini *et al.* (27) and Kang *et al.* (28), who said that the concentrated platelets in the fibrin matrix are biologically active proteins that support recruitment of cells from surrounding host tissue with stimulating growth factors and cell morphogenesis. It also shows a crucial role in the wound healing process and acts as a scaffold to bring the inflammatory cells, thus used for tissue regeneration and promoting bone healing. In group

no.3, there was a growth in callus mass size more than in the first group. This may be due to nano magnesium oxide, which was added to the fracture line in the third group because the nano magnesium oxide hastened bone healing, and this agreement with Hickey *et al.* (29), who said that the effects of adding nano-magnesium oxide to fracture bone showed significantly enhance adhesion and proliferation of osteoblast and suitable for bone applications with no cell toxicity.

The radiographic pictures of the tenth week after operation showed some progress in the bone remodeling process in all trial animals, but the bone remodeling was fastest in the second group than the other groups (first and third). Therefore, the fractured bone was more like a normal shape. The hastening of bone remodeling in this group may be due to added the platelets rich fibrin to the fracture line. This coincides with Hidajat *et al.*; Dülgeroglu, and Metineren (30,31), who said that the platelets rich in fibrin act as osteoconduction and osteoinduction, as well stimulates bone regeneration by activating osteoblast differentiation. Therefore, the bone remodeling occurred early in this group. Whereas the third group was progressed than the first group in bone remodeling, and this is may because added the nano-magnesium oxide to the fracture line, this is in the same line of Li *et al.* (13) and Wu *et al.* (32), who stated that the presence of magnesium ions plays a role in promoting osteogenic differentiation from mesenchymal stem cells; also stimulating adhesion, proliferation of osteogenic cells. As well as the biodegradable nano-magnesium oxide works to make the surrounding environment weakly alkaline, and this having a significant role in stimulating mineralization (calcium, phosphorous, and phosphate) of the new calculus formation during the bone healing process.

The results of total serum calcium concentrations rates in table 1 showed a significantly statistical difference between the first and the rest groups (second and third) for the second and fourth week after the operation, with no significant difference between the second and third groups at the same period. Also, there was no significant difference among the three trial groups for the sixth and eighth weeks after surgical operation. These results indicated that all experimental animals did not suffer from delayed union or osteoporosis, confirmed by radiographic pictures showing new callus formation with new bone formation (ossification). This coincided with Fischer *et al.* (33), who stated that calcium gives the bones strength and rigidity. Also, the bones act as a reservoir for calcium to maintain constant blood calcium levels. The alkaline phosphatase concentration rates showed an increase in the second group than the rest (first and third) at the sixth week after the operation. This increase indicates more osteoblast activity to form new callus formation, and this agrees with Singh *et al.* (34), who documented that the extraordinary rates of alkaline phosphatase in the blood serum indicate the activity of osteoblasts. This alkaline phosphatase leads to the new bone by the formation of the bone matrix and its mineralization.

Conclusion

This experimental study concluded that using platelets rich fibrin and nano magnesium oxide was beneficial for enhancing and improving radial bone fracture healing in dogs.

Acknowledgments

The authors of this work would like to show their profound thanks to the College of Veterinary Medicine, University of Mosul, for supporting the current study.

Conflict of interest

The authors declare that no conflict of interest exists.

References

- Mohsina A, Zama MMS, Tamilmahan P, Gugjoo MB, Singh K, Gopinathan A, Gopi M, Karthik K. A retrospective study on incidence of lameness in domestic animals. *Vet World*. 2014;7(8):601-604. DOI: [10.14202/vetworld.2014.601-604](https://doi.org/10.14202/vetworld.2014.601-604)
- Gwyneth KW, Noel MMM. Cuttable plate fixation for small breed dogs with radius and ulna fractures: Retrospective study of 31 dogs. *Can Vet J*. 2017;58(4):377-382. [\[available at\]](https://doi.org/10.1139/cv-2016-02-010)
- Brianza SZM, Delise M, Ferraris MM, D'Amelio P, Botti P. Cross-sectional geometrical properties of distal radius and ulna in large, medium, and toy breed dogs. *J Biomech*. 2006;39(2):302-311. DOI: [10.1016/j.jbiomech.2004.11.018](https://doi.org/10.1016/j.jbiomech.2004.11.018)
- Milovancev M, Ralphs C. Radius/Ulna fracture repair. *Clin Tech Small Anim Pract*. 2004;19(3):128-133. DOI: [10.1053/j.ctsap.2004.09.005](https://doi.org/10.1053/j.ctsap.2004.09.005)
- Mafamane H, Hackenbroich C, Ellinghaus A, Schmidt-Bleek K. Research in fracture healing and its clinical applications in the veterinary practice. *J Vet Sci Ani Husb*. 2017;5(3):2348-9790. DOI: [10.15744/2348-9790.5.303](https://doi.org/10.15744/2348-9790.5.303)
- Brannigan K, Griffin M. An update into the application of nanotechnology in bone healing. *Open Orthop J*. 2016;10(1):808-823. DOI: [10.2174/1874325001610010808](https://doi.org/10.2174/1874325001610010808)
- Qifei W, Jianhua Y, Junlin Y, Bingyun L. Nanomaterials promise better bone repair. *Mater Today*. 2016;19(8):451-463. DOI: [10.1016/j.mattod.2015.12.003](https://doi.org/10.1016/j.mattod.2015.12.003)
- Zhao-Gui Z, Zhi-Hong L, Xin-Zhan M, Wan-Chun W. Advances in bone repair with nano biomaterials: Mini-review. *Cytotechnol*. 2011;63:437-443. DOI: [10.1007/s10616-011-9367-4](https://doi.org/10.1007/s10616-011-9367-4)
- Kumar S, Gautam C, Chauhan BS, Srikrishna S, Yadav RS, Rai SB. Enhanced mechanical properties and hydrophilic behavior of magnesium oxide added hydroxyapatite nanocomposite: A bone substitute material for load-bearing applications. *Ceramics Inter*. 2020;46(10):16235-16248. DOI: [10.1016/j.ceramint.2020.03.180](https://doi.org/10.1016/j.ceramint.2020.03.180)
- Khandaker M, Li Y, Morris T. Micro and nano MgO particles for the improvement of fracture toughness of bone-cement interfaces. *J Biomech*. 2013;46(5):1035-1039. DOI: [10.1016/j.j.2012.12.006](https://doi.org/10.1016/j.j.2012.12.006)
- Tan CY, Yaghoubi A, Ramesh S, Adzila S, Purbolaksono J, Hassan MA, Kutty MG. Sintering and mechanical properties of MgO-doped nanocrystalline hydroxyapatite. *Ceramics Inter*. 2013;39(8):8979-8983. DOI: [10.1016/j.ceramint.2013.04.098](https://doi.org/10.1016/j.ceramint.2013.04.098)
- Banerjee SS, Tarafder S, Davies NM, Bandyopadhyay A, Bose S. Understanding the influence of MgO and SrO binary doping on the mechanical and biological properties of β -TCP ceramics. *Acta Biomaterial*. 2010;6(10):4167-4174. DOI: [10.1016/j.bio.2010.05.012](https://doi.org/10.1016/j.bio.2010.05.012)
- Li C, Sun J, Shi K, Long J, Li L, Lai Y, Qin L. Preparation and evaluation of osteogenic nano-MgO/PMMA bone cement for bone healing in a rat critical-size calvarial defect. *J Mater Chem B*. 2020;8(21):4575-4586. DOI: [10.1039/d0tb00074d](https://doi.org/10.1039/d0tb00074d)
- Coelho CC, Araújo R, Quadros PA, Sousa SR, Monteiro FJ. Antibacterial bone substitute of hydroxyapatite and magnesium oxide to prevent dental and orthopedic infections. *Materials Science and Engineering: C*. 2019;97:529-38. DOI: [10.1016/j.msec.2018.12.059](https://doi.org/10.1016/j.msec.2018.12.059)
- Naik B, Karunakar P, Jayadev M, Marshal VR. Role of Platelet-rich fibrin in wound healing: A critical review. *J Conserv Dent*. 2013;16(4):284-293. DOI: [10.4103/0972-0707.114344](https://doi.org/10.4103/0972-0707.114344)
- Motwani K, and Sharma K. Platelet-rich fibrin - a novel acumen into regenerative endodontic therapy. *Resto Dentist Endodon*. 2014;39(1):1-6. DOI: [10.5395/rde.2014.39.1.1](https://doi.org/10.5395/rde.2014.39.1.1)
- Singh A, Kohli M, Gupta N. Platelet-rich fibrin: a novel approach for osseous regeneration. *J Maxillofacial Oral Surg*. 2012;11(4):430-434. DOI: [10.1007/s12663-012-0351-0](https://doi.org/10.1007/s12663-012-0351-0)
- Anitua E, Sanchez M, Nurden AT, Nurden P, Orive G, Andía I. New insights into and novel applications for platelet-rich fibrin therapies. *Trend Biotechnol*. 2006;24(5):227-234. DOI: [10.1016/j.2006.02.010](https://doi.org/10.1016/j.2006.02.010)
- Kim TH, Kim SH, Sándor GK, Kim YD. Comparison of platelet-rich plasma (PRP), platelet-rich fibrin (PRF), and concentrated growth factor (CGF) in rabbit-skull defect healing. *Arch Oral Biol*. 2014;59(5):550-8. DOI: [10.1016/j.archoralbio.2014.02.004](https://doi.org/10.1016/j.archoralbio.2014.02.004)
- Davis VL, Abukabda AB, Radio NM, Witt-Enderby PA, Clafshenkel WP, Cairone JV, Rutkowski JL. Platelet-rich preparations to improve healing. Part I: Workable Options for Every Size Practice. *J Oral Implant*. 2014;40(4):500-510. DOI: [10.1563/aaid-joi-d-12-00104](https://doi.org/10.1563/aaid-joi-d-12-00104)
- Tomlin J, Peadar M, Langley-Hobbs S, Muir P. Radial carpal bone fracture in dogs. *J Ameri Ani Hospi Associa*. 2001;37(2):173-178. DOI: [10.5326/15473317-37-2-173](https://doi.org/10.5326/15473317-37-2-173)
- Bai M, Wang C, Wang J, Lin M, Chan W. Three-dimensional structure and cytokine distribution of platelet-rich fibrin. *Clin*. 2017;72(2):116-124. DOI: [10.6061/clinics/2017\(02\)09](https://doi.org/10.6061/clinics/2017(02)09)
- Dohan DM, Choukroun J, Diss A, Dohan SL, Dohan AJJ, Mouhyi J, Gogly B. Platelet-rich fibrin (PRF): A second-generation platelet concentrate. Part II: Platelet-related biologic features. *Oral Surg Oral Med Oral Pathol Oral Radiol Endod*. 2006;101(3):e45-e50. DOI: [10.1016/j.tripleo.2005.07.009](https://doi.org/10.1016/j.tripleo.2005.07.009)
- Griffin MF, Kalaskar DM, Seifalian A, Butler PE. An update on the application of nanotechnology in bone tissue engineering. *J Open Orthopae*. 2016;10(3):836-848. DOI: [10.2174/1874325001610010836](https://doi.org/10.2174/1874325001610010836)
- Khiste SV, Naik TR. Platelet-rich fibrin as a biofuel for tissue regeneration. *ISRN Biomaterials*. 2013;1-6. DOI: [10.5402/2013/627367](https://doi.org/10.5402/2013/627367)
- Wang Q, Yan J, Yang J, Li B. Nanomaterials promise better bone repair. *Mater Today*. 2016;19(8):451-463. DOI: [10.1016/j.2015.12.003](https://doi.org/10.1016/j.2015.12.003)
- Serafini G, Lopreiato M, Lollobrigida M, Lamazza L, Mazzucchi G, Fortunato L, Mariano A, Scotto d'Abusco A, Fontana M, De Biase A. Platelet rich fibrin (PRF) and its related products: Biomolecular characterization of the liquid fibrinogen. *J Clin Med*. 2020;9(4):1099. DOI: [10.3390/jcm9041099](https://doi.org/10.3390/jcm9041099)
- Kang YH, Jeon SH, Park JY, Chung JH, Choung YH, Choung HW, Kim ES, Choung PH. Platelet-rich fibrin is a bioscaffold and reservoir of growth factors for tissue regeneration. *Tissue Engin: Part A*. 2011;17(3-4):349-359. DOI: [10.1089/ten.tea.2010.0327](https://doi.org/10.1089/ten.tea.2010.0327)
- Hickey DJ, Ercan B, Sun L, Webster TJ. Adding MgO nanoparticles to hydroxyapatite-PLLA nanocomposites for improved bone tissue engineering applications. *Acta Biomaterial*. 2015;14:175-184. DOI: [10.1016/j.actbio.2014.12.004](https://doi.org/10.1016/j.actbio.2014.12.004)
- Hidajat NN, Mulyadi D, Chaidir MR, Dewang TH. Platelet-rich fibrin enhances fracture healing in tibial long bone: An experiment in rabbit. *Althea Med J*. 2020;7(4):187-93. DOI: [10.15850/amj.v7n4.1960](https://doi.org/10.15850/amj.v7n4.1960)
- Dülgeroglu TC, Metineren H. Evaluation of the effect of platelet-rich fibrin on long bone healing: An experimental rat model. *Orthop*. 2017;40(3):e479-e484. DOI: [10.3928/01477447-20170308-02](https://doi.org/10.3928/01477447-20170308-02)
- Wu Z, Meng Z, Wu Q, Zeng D, Guo Z, Yao J, Bian Y, Gu Y, Cheng S, Peng L, Zhao Y. Biomimetic and osteogenic 3D silk fibroin composite scaffolds with nano MgO and mineralized hydroxyapatite for bone regeneration. *J Tissue Eng*. 2020;11:1-21. DOI: [10.1177/420967791](https://doi.org/10.1177/420967791)
- Fischer V, Haffner-Luntzer M, Amling M, Ignatius A. Calcium and vitamin D in bone fracture healing and post-traumatic bone turnover. *Euro Cell Mater*. 2018;35:365-385. DOI: [10.22203/ECM.v035a25](https://doi.org/10.22203/ECM.v035a25)

34. Singh CK, Sarma KK, Kalita D, Tamuly S, Hussain J, Deuri B, Nath PJ. Haemato-biochemical, radiographic and clinical outcome in healing of femoral fracture with retrograde intramedullary pin in conjunction with demineralized bone matrix in dogs. J Exper Biol Agricult Scien. 2017;5(2):201-207. DOI: [10.18006/2017.5\(2\).201.207](https://doi.org/10.18006/2017.5(2).201.207)

دراسة مقارنة لنانو أكسيد المغنيسيوم مقابل الليفين الغني بالصفائح الدموية لإصلاح كسر عظم الكعبرة المستحدث في الكلاب

ياسر فارس عبدالموجود و ميسر غانم ذنون

فرع الجراحة وعلم تناسل الحيوان، كلية الطب البيطري، جامعة الموصل، الموصل، العراق

الخلاصة

أجريت هذه الدراسة لتقييم تأثيرات نانو أكسيد المغنيسيوم مقابل الليفين الغني بالصفائح الدموية على التئام الكسر المستحدث في عظم الكعبرة. تم استخدام ثمانية عشر من الذكور والإناث غير الحوامل من الكلاب المحلية الضالة، وبمعدل وزن $17,6 \pm 0,8$ كغم وبمعدل عمر $2,0 \pm 0,1$ سنة. قسمت حيوانات التجربة وبشكل عشوائي إلى ثلاث مجاميع متساوية. المجموعة الأولى، مجموعة السيطرة، تم إحداث الكسر المستعرض في عظم الكعبرة ومن ثم تم تثبيته عن طريق التثبيت الخارجي بوساطة الجبسونا، في هذه المجموعة لم يتم معالجة خط الكسر بأي مادة نشطة بيولوجيًا. المجموعة الثانية، مجموعة الليفين الغنية بالصفائح الدموية، تم معالجة خط الكسر في هذه المجموعة بإضافة الليفين الغني بالصفائح الدموية على خط الكسر. المجموعة الثالثة، مجموعة نانو أكسيد المغنيسيوم، في هذه المجموعة تمت معالجة خط الكسر بإضافة معلق من نانو أكسيد المغنيسيوم. أظهرت نتائج التصوير الشعاعي أن التئام العظم المكسور كان الأسرع في المجموعة الثانية مقارنة بالمجموعتين الأولى والثالثة، بينما كانت المجموعة الثالثة أفضل من المجموعة الأولى. زادت معدلات تراكيز الكالسيوم والفوسفاتيز القلوي في الأسابيع التي أعقبت العملية الجراحية. اعتمادًا على الصور الشعاعية والمعدلات التسلسلية لإنزيم الفوسفاتيز القلوي، كانت المجموعتان الثانية والثالثة هما الأفضل شفاءً للعظام المكسورة من المجموعة الأولى. وفي الختام، أوضحت نتائج هذه الدراسة أن استخدام كل من الليفين الغني بالصفائح الدموية ونانو أكسيد المغنيسيوم عزز وحسن من شفاء الكسر المستحدث في عظم الكعبرة.